J Fluoresc (2015) 25:31–38
DOI 10.1007/s10895-014-1451-7

ORIGINAL PAPER

Cetyltrimethylammonium Bromide Capped 9-Anthraldehyde Nanoparticles for Selective Recognition of Phosphate Anion in Aqueous Solution Based on Fluorescence Quenching and Application for Analysis of Chloroquine

Prasad G. Mahajan · Netaji K. Desai · Dattatray K. Dalavi · Dhanaji. P. Bhopate · Govind B. Kolekar · Shivajirao R. Patil

Received: 24 June 2014 / Accepted: 4 September 2014 / Published online: 21 September 2014

Abstract Cetyltrimethylammonium bromide (CTAB) capped 9-Anthraldehyde nanoparticles (9-AANPs) in aqueous suspension prepared by reprecipitation method are seen brick shaped in Scanning Electron Microscope image. The Dynamic Light Scattering histogram of nanoparticle suspension reveals narrow particle size distribution and average particle size is 89 nm. The positive zeta potential 20.8 mV measured on zeta sizer indicates high level stability of nanoparticle suspension. The blue shift of 65359.47 cm^{-1} observed in the UV-Visible absorption spectrum of CTAB capped 9-AANPs from the absorption maximum of dilute solution of 9-Anthraldehyde (9-AA) in acetone is an indication of formation of H-bonded aggregates by π stacking effect. The strong Aggregation Induced Enhanced Emission (AIEE) of CTAB capped 9-AANPs at 537 nm is selectively quenched with addition of phosphate anion solution. The fluorescence quenching results of the nanoparticle in aqueous solution fit into conventional Stern–Volmer relation in the range of phosphate ion concentration of 0–40 μM. The possible mechanism of fluorescence quenching of nanoparticle is explained by considering adsorption of phosphate anion electrostatistically on positively charged surface of nanoparticle generated by CTAB cap. The Langmuir adsorption plot constructed for PO_4^{3-} adsorption on the basis of fluorescence quenching results of CTAB capped 9-AANPs is linear. The estimated value of Langmuir constant (K) and Stern – Volmer constant (K_{sv}) are in close agreement within experimental limits. The sensing method of phosphate ion based on fluorescence quenching of 9-AANPs is applied successfully for quantification of phosphate from pharmaceutical tablet chloroquine phosphate and hence to determine the amount of chloroquine.

Keywords 9-Anthaldehyde nanoparticles · Cetyltrimethylammonium bromide · Fluorescence quenching · Phosphate anion sensing · Langmuir adsorption · Chloroquine

P. G. Mahajan · N. K. Desai · D. K. Dalavi · D. P. Bhopate · G. B. Kolekar · S. R. Patil (✉)
Fluorescence Spectroscopy Research Laboratory, Department of Chemistry, Shivaji University, Kolhapur 416 004, Maharashtra, India
e-mail: srp_fsl@rediffmail.com

S. R. Patil
e-mail: srp_chem@unishivaji.ac.in

Introduction

Fluorescent organic nanoparticles (FONs) have attracted attention due to selective binding character with analyte molecules [1–3]. FONs have inspired growing research efforts due to great diversity of organic molecules available, the flexibility in material synthesis, good water solubility and optical properties [4–6]. The absorption and fluorescence spectral properties are special due to effect of the charge transfer exciton formation with increased surface to volume ratio [7], multiple and enhanced emission [8, 9]. Inorganic materials and metal nanoparticles are reported [10, 11] successively in recent years but least attempts have been made to design and characterize the fluorescent organic nanoparticles. The methods of preparation of inorganic and metal nanoparticles are lengthy, complicated and expensive. In contrast preparation of fluorescent organic nanoparticles is simple, quick and cost effective method [12–14]. Recent reports are available on the studies of fluorescent organic nanoparticles for detection of Ag^+ in aqueous media [15], globulin in human serum [16], and

complex secondary sensor for cysteine [17], nucleic acids [18], divalent copper in aqueous media [19]. Functionalized and surface modified organic nanoparticles exhibiting strong aggregation induced enhanced emission (AIEE) are exploited as sensors working on Off/On fluorescence switching [20–22]. The micelle solution of substituted Polynuclear aromatic hydrocarbons (PAHs) and their functionalized derivatives are widely used as probes for the detection of vitamin B_2 and proflavin hemisulphate based on fluorescence quenching technique [23, 24]. It is known that water insoluble organic molecules having pair of non-bonded electron with heteroatom and electropositive hydrogen atom in functional moiety on phenyl ring can undergo hydrogen bonding in aqueous medium to form dimer. The careful nucleation in aqueous medium of such compounds from their homogeneous solution in volatile solvent can give nanoparticles due to aggregation. Hence, with a hope to obtain nanoparticles exhibiting AIEE the fluorescent 9-Anthraldehyde (9-AA) was chosen for preparation of nanoaggregates by reprecipitation method and as per expectation aqueous suspension of nanoparticles exhibiting red shifted enhanced emission was achieved. The positive zeta potential value 20.8 mV measured by Dynamic Light Scattering (DLS) Zeta Sizer indicating the surface functionality of nanoparticles can attract electrostatically the negatively charged analyte species. Itwas found that phosphate anion undergoing binding with nanosurface can be recognized by measuring changes in fluorescence of surface modified nanoparticles.

Phosphate is a key building block for enzymes, nucleic acids, phospholipids and nucleoproteins which are important intracellular compounds in the human body metabolism. The primary role of phosphate is to help to form strong bones and teeth in the human body. Organic phosphates are important in biochemistry, biogeochemistry or ecology (http://en.wikipedia.org/wiki/Phosphate, http://www.wales.nhs.uk/sitesplus/documents/864/wkplsite.pdf). The organic chloroquine phosphate is an antimalarial drug [25] and recently became popular as an agent in the treatment of chronic chikunguniya arthritis [26]. Chloroquine possesses two basic ionization sites with pKa values of 8.1 and 10.4 [27]. Hence, dicationic conjugated acid chloroquine forms phosphate salt by attaching with negatively charged oxygen atoms of conjugate base H_3PO_4. It is freely soluble in water and hence rapidly and almost completely absorbed from the gastro-intestinal tract when taken orally. The proportion of chloroquine diphospahte salt [7- chloro-4 (4- diethyl-amino-L-methylamino) quinoline, $2H_3PO_4$] is 1:2. Acute overdose of chloroquine in human body is extremely dangerous and death can occur within few hours [28]. Consequently, the quantitative determination of chloroquine in biological samples and medicinal tablets is of current interest. The method of sensing of phosphate can be used to determine chloroquine from pharmaceutical formulation. The methodologies used for the detection of phosphate anion are Colorimetry, Potentiometry, Amperometry, Conductometry and Voltammetry [29]. However, these methods require appreciable concentration of analyte and fail to detect when phosphate is in trace level. Recently direct fluorimetry and fluorescence sensing method using receptors are reported [30, 31]. The conventional receptors used so far are aminoimidazolium [32], dinuclear zinc based complex with terpyridine and tetraazacyclododecan [33] and protein incorporated within nanoparticles [34]. However, direct fluorimetry requires prior separation of analyte and in sensing, synthesis methods of receptors involve complicated and time consuming routes. The highly fluorescent organic 9-anthraldehyde nanoparticles (9-AANPs) with surface modified by Cetyltrimethylammonium bromide (CTAB) capping seen to sense PO_4^{3-} anion by complexation without using expensive receptors and exhibited quenching of fluorescence of aqueous suspension of nanoparticles. The present paper reports preparation and characterization of surface modified 9-AANPs to explore as sensor for phosphate in aqueous solution and application to determine chloroquine from pharmaceutical tablet based on fluorescence quenching even in presence of other ingredients used in formulation of tablet.

Experimental

Materials

9-Anthraldehyde (9-AA), Phosphoric acid obtained from Sigma Aldrich (India) andCetyltrimethylammonium bromide (CTAB) procured from Spectrochem Pvt. Ltd. Mumbai, (India) were used as received. Analytical grade acetone (S. D. Fine Chemicals, Mumbai, India) was used after distillation. Ultrapure water was obtained by passing distilled water through a Millipore unit (India) and used in preparation of solution required for fluorescence quenching experiments.

Preparation of CTAB stabilized 9-AANPs

A simple, quick and efficient reprecipitation method [12–14] was developed in the laboratory to prepare nanoparticles of 9-AA. 2 mL solution of 9-AA in acetone (1 mM) was injected into 100 mL aqueous solution of CTAB (20 mM) by using micro syringe. The whole solution was vigorously stirred by magnetic stirrer for 1 h and sonicated for 15 min at 30 °C to disperse the nanoparticles in aqueous layer. The main function of CTAB is to stabilize the 9-AANPs and also, to create a positive charge density over the surface of nanoparticles [3]. Yellow colored transparent suspension of nanoparticles was undertaken further for particle size distribution and surface morphology studies. The suspension of nanoparticles was also prepared by changing concentration of sample solution and surfactant solution. The suspension showing narrow particle

size distribution in DLS histogram and monodispersity was selected for photophysical and fluorescence quenching experiments.

Characterization Techniques

The particle size distribution and zeta potential of 9-AANPs was measured using a Malvern Zeta Sizer (Nano ZS-90) equipped with 4Mw, 633 nm He-Ne Laser (U.K.) at 25 °C under a fixed angle of 90^0 in disposable polystyrene cuvettes. The steady state fluorescence spectra of the aqueous suspension of 9-AANPs monitored at its excitation wavelength was recorded on Spectrofluorometer (JASCO, Japan, Model FP-8300). The excitation wavelength 265 nm was obtained from the excitation spectrum and the emission spectrum was monitored at this excitation wavelength. Absorption spectra were measured using a UV-3600 UV-visible-NIR Spectrophotometer (Shimadzu, Japan). A Scanning Electron Microscope, (SEM) (JEON-6360 Japan) was used to examine the morphology and size of the nanoparticles.

Results and Discussion

Particle Size and Morphology of CTAB capped 9-AANPs

Fig. 1(a) shows particle size distribution histogram of aqueous suspension of 9-AANPs recorded on DLS equipment and Fig. 1(b) is microphotograph of air dried film of aqueous suspension of 9-AANPs taken on SEM equipment. The histogram shows the remarkably narrow size distribution and the average diameter of the nanoparticles is 89 nm. The SEM

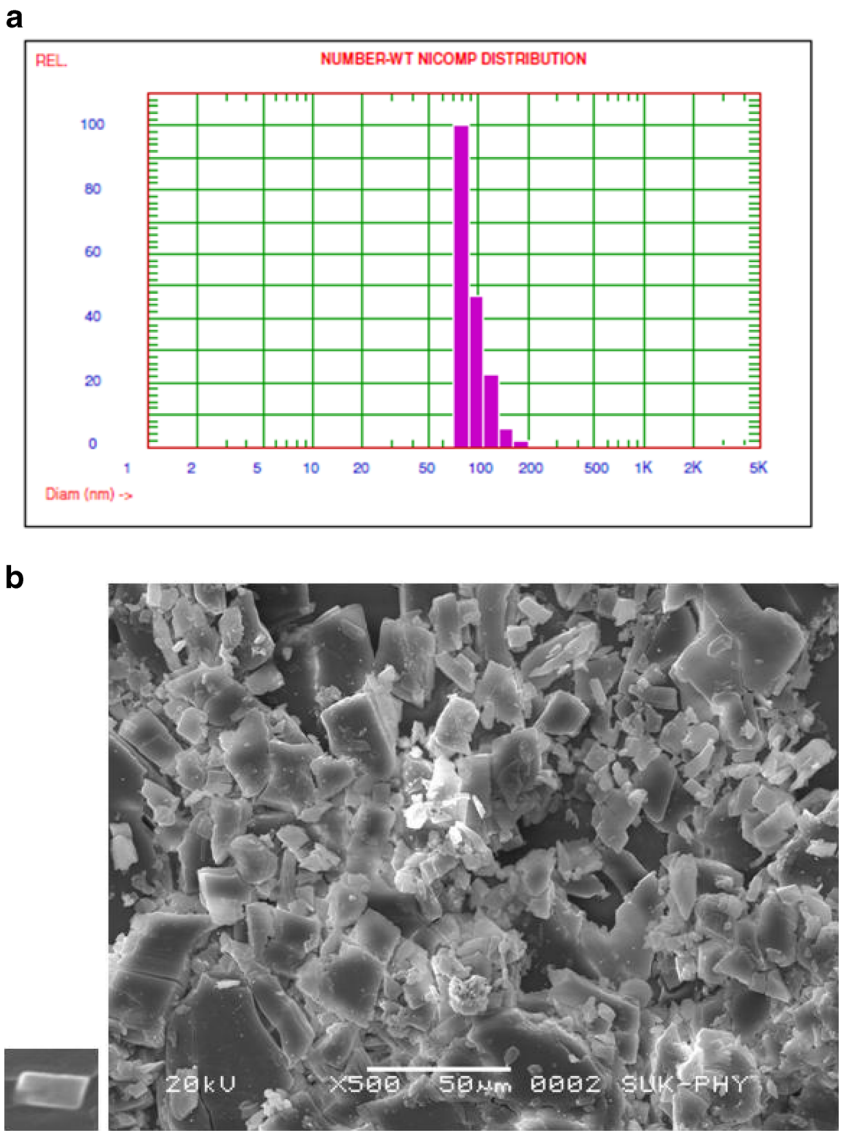

Fig. 1 **a** Particle Size Distribution Histogram of CTAB capped 9-AANPs obtained by DLS analysis, **b** SEM photomicrograph of air dried layer of CTAB capped 9-AANPs

image shows distinct brick shaped nanoparticles and average particle size is 500 nm. The greater size shown by SEM microphotograph is because of aggregation of nanoparticles into cluster during film formation on the glass substrate by evaporation of water. The zeta potential measured by DLS-Zeta Sizer is 20.8 mV. The value of zeta potential in the range from −25 mV to +25 mV is an indicative of higher level stability of nanoparticle suspension.

Photophysical Properties of CTAB capped 9-AANPs

Formation of nanoparticles in aqueous suspension is further confirmed by absorption and fluorescence spectroscopy. Fig. 2 presents absorption spectra of dilute solution of 9-AA in acetone (A) and aqueous suspension of 9-AANPs (B). Absorption spectra of dilute sample solution of 9-AA is broad band peaking at 405 nm while that of 9-AANPs show blue shifted structured sharp bands at 252 nm and 262 nm. The observed blue shift and structured absorption spectrum indicates that the 9-AA molecule aggregates in planar cluster. The fluorescence excitation and emission spectra of 9-AA in acetone and 9-AANPs suspension are shown in Fig. 3. It is seen that the excitation spectrum of nanoparticles is structured and spectrally identical with absorption spectrum. The structured spectrum is an indication of planarization of monomers and the hence anthryl moiety and substituent –CHO are considered to exist in the same plane in nanoaggeregates. However, the structureless, broad absorption and excitation spectrum of dilute solution of sample molecules indicates that the anthryl and substituent –CHO are coplanar, exhibits wider spectral separation in their maxima. The absorption transition $S_0 \longrightarrow S_1$ is $\pi \longrightarrow \pi^*$ because of conjugated phenyl rings and more number of delocalized π electrons. In contrast, the absorption spectrum of nanoparticle suspension is blue shifted from absorption spectrum of sample solution. The structured spectrum with absorption band at 252 nm and 262 nm led us to consider the contribution of individual molecules. The large

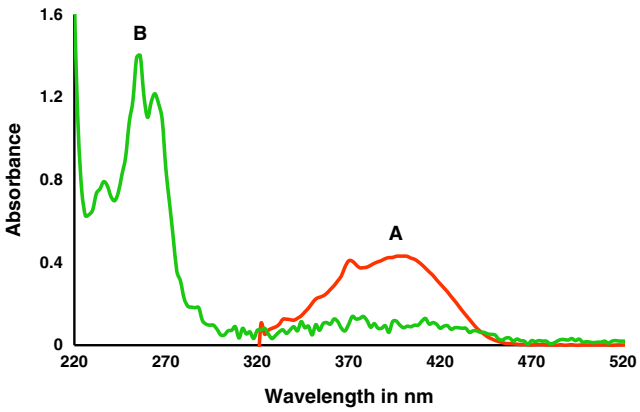

Fig. 2 Absorption Spectra of CTAB capped 9-AANPs (Spectrum B) and solution of 9-AA in acetone (Spectrum A)

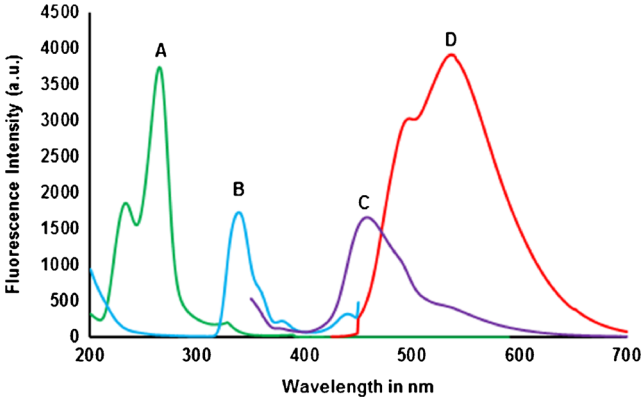

Fig. 3 Excitation spectra of CTAB capped 9-AANPs suspension (A) and of dilute solution of 9-AA in acetone (B) and Fluorescence Spectra of CTAB capped 9-AANPs suspension (D) and dilute solution of 9-AA in acetone (C)

blue shift in the absorption spectrum further indicates that the H-type aggregates are formed due to strong lateral π-stacking interaction [21] of anthryl structure in the hydrophobic core of micelle while polar –CHO functional moiety points outward towards aqueous phase. The fluorescence spectrum of 9-AANPs aqueous suspension shown in Fig. 3 is a broad, structureless band having enhanced emission at 537 nm and bathochromically shifted by 11449.412 cm^{-1} from the isolated emission of single molecule (monomer) in acetone seen at 458 nm. The monomer emission peak is not seen in the spectrum of nanoparticle suspension. The emission spectrum of nanoparticle also shows high energy weak band at 498 nm which is assigned to the less probable $\pi^* \longrightarrow n$ transition due to polar C=O group. The strong enhanced emission at 537 nm is assigned to the most probable $\pi^* \longrightarrow \pi$ transition owing to face-face π stacking effect in nanoaggregates. The dipole-dipole interaction between closely stacked neighboring molecules in H- aggregates cause the electronic transition dipoles of each monomer to arrange parallel to one another based on a gradual increase in the excitonic coupling effect by which the exciton relaxes to an energetically lower lying excited state. It is therefore believed that the emission originate from lower lying excited state of nanoaggregate than the excited state of isolated 9-AA molecule in solution and thus the nano emission is bathochromically shifted [3]. The Stokes shift estimated as a difference between excitation and emission maxima in nanoparticles suspension ($\Delta\bar{\upsilon}$=19113.875 cm^{-1}) which is higher than that of 9-AA solution in acetone ($\Delta\bar{\upsilon}$= 7664.463 cm^{-1}). The larger Stokes Shift is evidence of strong intermolecular forces due to in plane aggregation of molecules in nanoaggregates. The low emission intensity in solution of isolated molecule is due to dissipation of energy for molecular rotation. However, enhanced emission in nanoaggregates is because of the molecular rotations hindered by adjacent molecules and the restricted nonradiative decay thus favors radiative pathway of excited nanoaggregates [35].

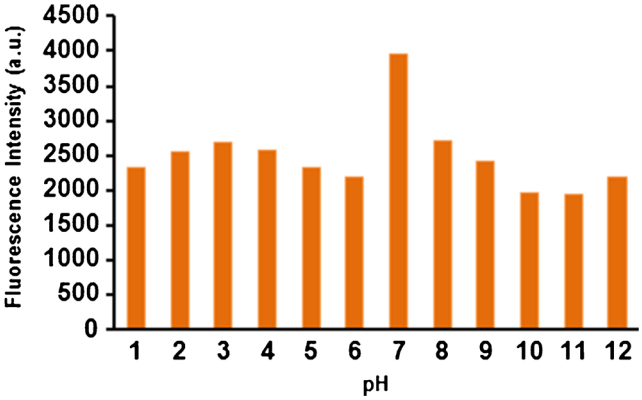

Fig. 4 Effect of pH on fluorecsence intensity of CTAB capped 9-AANPs suspension. (λem=537 nm and λex=265 nm)

Effect of pH on fluorescence intensity of CTAB capped 9-AANPs

The intensity of AIEE [20–22] of CTAB stabilized NPs of 9-AA was affected by pH changes of aqueous suspension. Hence effect of pH on the intensity of fluorescence in aqueous suspension of NPs has been studied. The bar diagram illustrating the effect of pH on intensity of fluorescence is shown in Fig. 4. The maximum fluorescence intensity seen at pH=7 indicates high power colloidal stability at this pH. At low and high pH the colloidal stability is affected by disruption of the CTAB cage resulting in lowering of fluorescence intensity due to disaggregation of nanoparticles.

Sensing Property of CTAB capped 9-AANPs in selective recognition of PO_4^{3-} ion

The positive zeta potential 20.8 mV of CTAB capped 9-AANPs in aqueous suspension indicates its ability to bind anions. Hence the addition of solution of salts of anion in the aqueous suspension may produce changes in the absorption and fluorescence property. The fluorescence response of nanoparticle in aqueous suspension was examined in the presence of solution of different anions like PO_4^{3-}, Br^-, CH_3COO^-, ClO^-, BrO_3^-, $S_2O_8^{2-}$, I^- of concentration 20 μM each. Fig. 5 is the bar diagram of fluorescence intensity change $\frac{F_0-F}{F}$ where, F_0 and F are the fluorescence intensity of nanoparticle in absence and presence of anion measured at wavelength 537 nm. It is seen that the decrease in fluorescence intensity is significant for PO_4^{3-}anion (Fig. 5. Red bar diagram) whereas other anions do not respond to produce appreciable changes in the fluorescence intensity of 9-AANPs. The fluorimetric titration was carried out by adding increasing amounts of phosphate ion solution at pH=7 using phosphate buffer. Fig. 6 shows fluorescence spectra of aqueous suspension of 9-AANPs in presence of PO_4^{3-} ion solution in the concentration range from 0 to 40 μM measured at room temperature. The fluorescence intensity of nanoparticles decreases regularly without any spectral shift. The quenching data was analyzed by using conventional Stern-Volmer relation.

$$\frac{F_0}{F} = 1 + K_{SV}[Q] \tag{1}$$

where, F and F_O are the fluorescence intensity of 9-AANPs at a given PO_4^{3-} anion solution of concentration [Q] and PO_4^{3-} anion free solution respectively. The Stern–Volmer plot presented in Fig. 7 reveals good linear relationship and coefficient of linear fit (R^2) is 0.994. The estimated value of Stern-Volmer constant (K_{sv}) from slope of the straight line is 0.062×10^5 M^{-1}. The limit of detection determined by the equation,

$$LOD = \frac{3.3\sigma}{k} \tag{2}$$

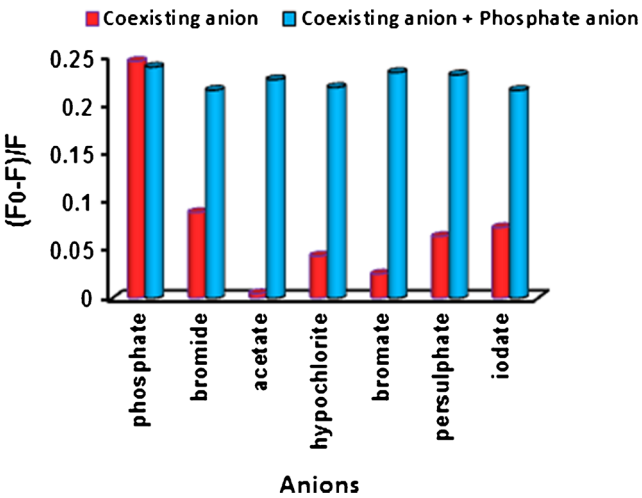

Fig. 5 Bar diagram showing fluorescence Intensity response [$(F_0-F)/F$] of CTAB capped 9-AANPs in the presence and absense of the PO_4^{3-} ion and several coexisting anions like Br^-, CH_3COO^-, ClO^-, BrO_3^-, $S_2O_8^{2-}$, I^- solutions of 20 μM concentrations (λex=265 nm)

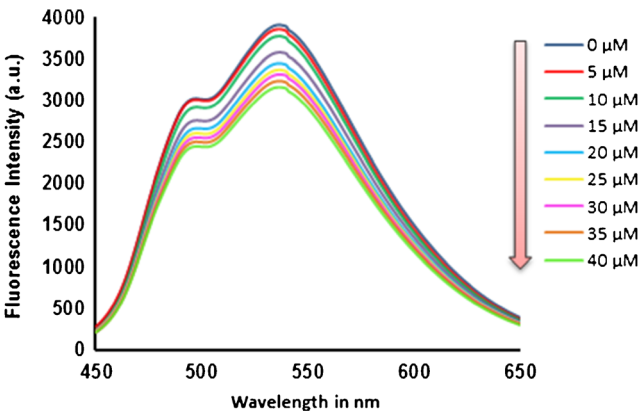

Fig. 6 Fluorescence Spectra of CTAB capped 9-AANPs suspension (1×10^{-6} M) in the presence of different concentrations of PO_4^{3-} ions (0, 5, 10, 15, 20, 25, 30, 35 and 40 μM)

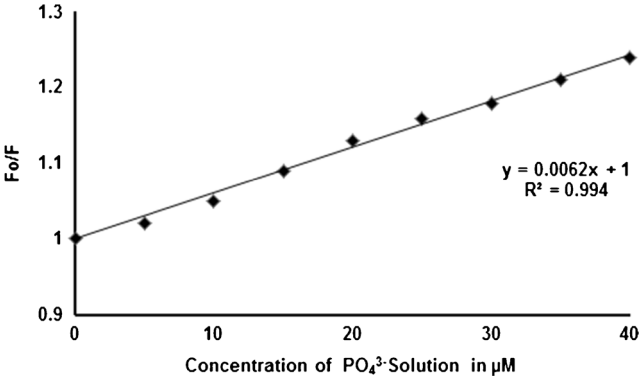

Fig. 7 Stern- volmer plot of fluorescence quenching data of CTAB capped 9-AANPs upon addition of different amounts of PO_4^{3-} ion solution

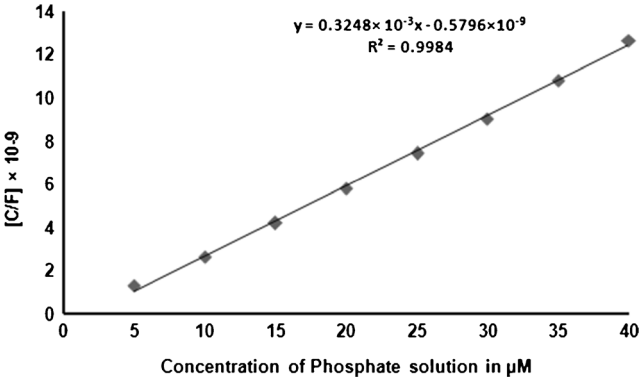

Fig. 8 Plot of $\frac{C}{F}$ as a function of concentration (C) of PO_4^{3-} (Langmuir Adsorption Plot)

is 7.563×10^{-5} M, where σ is the standard deviation of the y- intercepts of the regression lines and *k* is the slope of the calibration graph.

Mechanism of binding and fluorescence quenching

PO_4^{3-} anions are believed to be adsorbed and bind with positively charged surface of 9-AANPs by electrostatic forces of attraction between them, because of the tetrahedral structure of phosphate carrying negative charges on the three oxygen atoms. The rate of binding of PO_4^{3-} to the nanoparticle surface (R_b) is proportional to its concentration 'C' in the analyte solution and the fraction of available binding sites is (1− θ); where θ is defined as the fraction of occupied states.

$$R_b = K_b(1-\theta) \tag{3}$$

Similarly, the rate of desorption of bound PO_4^{3-} from the nanoparticle surface depends only on the fraction of the occupied binding sites and expressed as,

$$R_d = K_d \tag{4}$$

At equilibrium, the rate of binding is equal to rate of desorption

$$K_d\theta = K_b(1-\theta) \tag{5}$$

where, K_b and K_d are the binding and desorption constant of phosphate anion.

The equation can be solved for a function of the ratio $B = \frac{K_b}{K_d}$

$$\theta = \frac{BC}{1+BC} \tag{6}$$

The fraction of occupied binding sites θ is related to the ratio of the fluorescence signal obtained (F) at given PO_4^{3-} concentrationand the maximum fluorescence intensity (F_0) without PO_4^{3-} solution as,

$$\theta = \frac{F}{F_0} = \frac{BC}{1+BC} \tag{7}$$

The equation can linearized to take the form,

$$\frac{C}{F} = \frac{1}{BF_0} + \frac{1}{F}C \tag{8}$$

The equation No. 8 is the linear form of Langmuir adsorption equation. Linearized plot of C/F Vs. Concentration of PO_4^{3-} (C) is shown in Fig. 8. The adsorption equilibrium constant B is the Langmuir binding constant (K) given by the slope and the intercept of the linear plot. Hence according to the Langmuir adsorption description [17, 19] the binding of PO_4^{3-} on the surface of nanoparticles can be examined by the plot of C/F as a function of concentration (C) of PO_4^{3-} and as per the expectation this plot shown in Fig. 8 is linear.

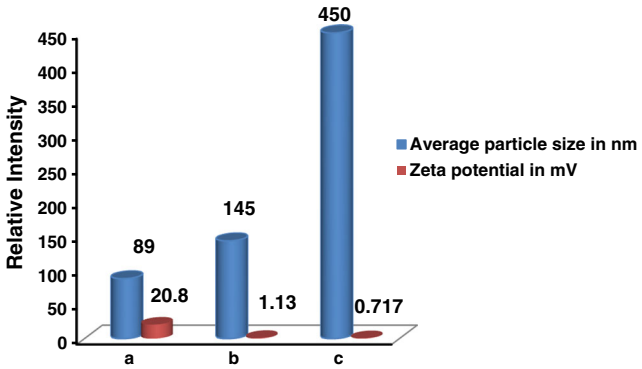

Fig. 9 Bar diagram showing variation of zeta potential and size of CTAB capped 9-AANPs (1×10^{-6} M) **a** in absence of PO_4^{3-} ion solution and **b** and **c** in presence of 20 μM and 40 μM PO_4^{3-} ion solution

Table 1 Determination of chloroquine phosphate and chloroquine in pharmaceutical sample

Sample	Composition	Amount of Chloroquine Phosphate in mg (Per Tablet)		Recovery	RSD	Amount of Chloroquine in mg (Per Tablet)		Recovery	RSD
		Certified	Found[a]			Certified	Found[a]		
Lariago Tablet, IpcaLaboratories Ltd, Sejvata, Ratlam, Madhya Pradesh, India.	Chloroquine Phosphate- 250 mg, Titanium dioxide IP, Calcium Stearate, Colloidal silicon dioxide, dibasic calcium phosphate, microcrystalline cellulose, Talc.	250	249.05	99.62 %	0.1421 %	155	154.41	99.61 %	0.1426 %

[a] Estimated value of chloroquine phosphate/chloroquine is average of five determinations

Coefficient of linear fit is 0.9984 and Langmuir binding constant K is 5.603×10^5 M^{-1}which could be considered as quenching constant. The adsorption results led to consider that the quenching of fluorescence of 9-AANPs is because of binding of adsorbed PO_4^{3-}.

In addition to this, the results of DLS-Zeta Sizer are supporting to the adsorption of phosphate ion over nanoparticle surface. Fig. 9 is the bar diagram showing variation of zeta potential and size of 9-AANPs in presence of PO_4^{3-} solution. It is seen that the zeta potential of the nanoparticle / water interface decreases from 20.8 mV to 1.13 mV and 0.717 mV and the particle size increases from 89 nm to 145 nm and 450 nm upon addition of 20 μM and 40 μM solution of phosphate ion respectively. These observations suggested that the adsorption of phosphate ion over the positively charged surface of nanoparticles reduces the possible radiative emission from the aggregated nanoparticles and results in the quenching of fluorescence intensity of 9-AANPs [36].

Application of PO_4^{3-} sensing method for quantification of chloroquine

The fluorescence quenching of CTAB capped 9-AANPs by phosphate anion was successfully applied for analysis of chloroquine from pharmaceutical tablet Lariago, made available commercially in the market by Ipca Laboratories Ltd, Sejvata, Ratlam, Madhya Pradesh (India). The composition of tablet is chloroquine phosphate 250 mg equivalent to 155 mg chloroquine base. Chloroquine and other ingredients like titanium dioxide IP, Calcium stearate, colloidal silicon dioxide, cellulose, talc used in formulation do not interfere because of the selectivity of positively charged surface of 9-AANPs towards phosphate anion only. The ratio of the fluorescence intensity of nanoparticles without solution of tablet (F_0) to the fluorescence intensity in presence of solution of tablet (F) was measured. Using Stern-Volmer plot in Fig. 7 as calibration graph, the quantity of phosphate in the solution of tablet of known volume was obtained and finally amount of chloroquine was calculated from the molecular formula of salt of chloroquine phosphate [$C_{18}H_{26}ClN_3$•$2H_3PO_4$]. The estimated amounts of chloroquine phosphate and chloroquine listed in Table 1 reveals that the proposed method is in good agreement with certified values and experimental values. The fluorescence quenching method has good repeatability. The average recovery is 99.61 % and R.S.D. is 0.1426 % for chloroquine in medicinal tablet. Therefore proposed method can be used safely for determination of chloroquine from tablet in aqueous solution without any pretreatment.

Conclusion

CTAB capped 9-AANPs in aqueous suspension were prepared by reprecipitation method to recognize phosphate anion. The SEM microphotograph of air dried film of 9-AANPs shows brick shaped particles while DLS histogram revealed narrow particle size distribution. The UV-Visible absorption and fluorescence spectroscopy results indicated the H- bonded aggregates involving π-stacking and strong AIEE is arising due to hindered molecular rotations favoring radiative decay of nanoaggregates. The results of fluorescence quenching of 9-AANPs by phosphate fits into Stern-Volmer relation and applied successfully to determine chloroquine from pharmaceutical tablet Lariago containing organic chloroquine phosphate, an antimalarial drug. The organic nanoparticles exhibiting Aggregation Induced Emission (AIE) in the Near-Infra Red (NIR) region are shown to be the better candidates for cell imaging. The fluorescence probe 9-AANPs emitting in the region 530–550 nm with maximum at 537 nm limits its use for the cell imaging because of interference with the body cell optical absorption, light scattering and auto fluorescence of biological media. However, the 9-AANPs conjugated with aromatic or aliphatic molecules like ketones, aldehydes, thiosemicarbazones, etc. can emit in NIR region and in its aggregated nano form will be a promising probe for cell imaging.

Acknowledgements The authors are grateful to the Department of Science and Technology (DST), New Delhi for providing funds under FIST-Level-II program for infrastructure improvement and University Grants Commission (UGC), New Delhi for financial support through DRS - Phase- II program to the Department of Chemistry, Shivaji University, Kolhapur.

References

1. Li X, Xu J, Yan H (2009) Ratiometric fluorescent determination of cysteine based on organic nanoparticles of naphthalene–thiourea–thiadiazole-linked molecule. Sensors Actuators B139:483–487
2. Singh A, Raj T, Aree T, Singh N (2013) Fluorescent organic nanoparticles of biginelli-based molecules: recognition of Hg^{2+} and Cl^{-}in an aqueous medium. Inorg Chem 52:13830–13832
3. Bhopate DP, Kolekar GB, Garadkar KM, Patil SR (2013) Cetyltrimethylammonium bromide stabilized perylenenanoparticles forfluorimetric estimation of bicarbonate (HCO^{3-}) anion: spectroscopic approach. Anal Methods 5:5324–5330
4. Yan H, Li H (2010) Urea type of fluorescent organic nanoparticles with high specificityfor HCO^{3-}Anions. Sensors Actuators B148:81–86
5. Fu H, Yao J (2001) Size effects on the optical properties of organic nanoparticles. J Am Chem Soc 123:1434–1439
6. Horn D, Rieger J (2001) Organic nanoparticles in the aqueous phase–theory, experiment, and Use. Angew Chem Int Ed 40:4330–4361
7. Ito F, Kakiuchi T, Sakano T, Nagamura T (2010) Fluorescence properties of pyrene derivative aggregates formed in polymer matrix depending on concentration. Phys Chem Chem Phys 12:10923–10927
8. Fu H, Loo B, Xiao D, Xie R, Ji X, Yao J, Zhang B, Zhang L (2002) Multiple emissions from 1,3-diphenyl-5-pyrenyl-2-pyrazoline nanoparticles: evolution from molecular to nanoscale to bulk materials. Angew Chem Int Ed 41(6):962–965
9. An B, Kwon S, Jung S, Park SY (2002) Enhanced emission and its switching in fluorescent Organic Nanoparticles. J Am Chem Soc 124:14410–41415
10. AlQahtani H, Sugden M, Puzzovio D, Hague L, Mullin N, Richardson T, Grell M (2011) Highly sensitive alkane odour sensors based on functionalised gold nanoparticles. Sensors Actuators B160: 399–404
11. Tautzenberger A, Kreja L, Zeller A, Lorenz S, Schrezenmeier H, Mailänder V, Landfester K, Ignatius A (2011) Direct and indirect effects of functionalized fluorescence-labelled nanoparticles on human osteoclast formation and activity. Biomaterials 32:1706–1714
12. Kasai H, Nalwa H, Oikawa H, Okada S, Matsuda H, Minami N, Kakuta A, Ono K, Mukoh A, Nakanishi H (1992) A novel preparation method of organic microcrystals. Jpn J Appl Phys 31:L1132
13. Kasai H, Kamatani H, Okada S, Oikawa H, Matsuda H, Nakanishi H (1996) Size dependent colors and luminescences of organic microcrystals. Jpn J Appl Phys 35:L221
14. Jinshui L, Lun W, Feng G, Yongxing L, Yun W (2003) Novel fluorescent colloids as a DNA fluorescence probe. Anal Bioanal Chem 377:346–349
15. Qu F, Liu J, Yan H, Peng L, Li H (2008) Synthesis of organic nanoparticles of naphthalene–thiourea–thiadiazole-linked molecule as highly selective fluorescent and colorimetric sensor for Ag(I). Tetrahedron Lett 49:7438–7441
16. Wang L, Wang L, Dong L, Bian G, Xia T, Chen H (2005) Direct fluorimetric determination of γ-globulin in human serum with organic nanoparticle biosensor. Spectrochim Acta A 61:129–133
17. Yan H, Su H, Tian D, Miao F, Li H (2011) Synthesis of triazolothiadiazole fluorescent organic nanoparticles as primary sensor toward Ag^{+} and the complex of Ag^{+}as secondary sensor toward cysteine. Sensors Actuators B160:656–661
18. Wang L, Xia T, Wang L, Chen H, Dong L, Bian G (2005) Preparation and application of a novel core-shell organic nanoparticle as a fluorescence probe in the determination of nucleic acids. Microchim Acta 149:267–272
19. Hou J, Wang L, Li D, Wu X (2011) A rigid conjugated pyridinylthiazole derivative and its nanoparticlesfor divalent copper fluorescent sensing in aqueous media. Tetrahedron Lett 52:2710–2714
20. An B, Lee D, Lee J, Park Y, Song H, Park SY (2004) Strongly fluorescent organogel system comprising fibrillar self-assemblyof a trifluoromethyl-based cyanostilbene derivative. J Am Chem Soc 126: 10232–10233
21. Lim S, An B, Jung S, Chung M, Park SY (2004) Photoswitchable organic nanoparticles and aPolymer film employing multifunctional molecules with enhanced fluorescence emissionand BistablePhotochromism. Angew Chem Int Ed 43:6346–6350
22. Zhang X, Zhang X, Wang S, Liu M, Tao L, Wei Y (2013) Surfactant modification of aggregation-induced emission material as biocompatible nanoparticles: facile preparation and cell imaging. Nanoscale 5:147–150
23. Bhattar SL, Kolekar GB, Patil SR (2008) Fluorescence resonance energy transfer between perylene and riboflavin in micellar solution and analytical application on determination of vitamin B_2. J Lumin 128:306–310
24. Patil DT, Mokashi VV, Kolekar GB, Patil SR (2013) Micellar-mediated binding interaction betweenproflavinehemisulfate and salicylic acid: Spectroscopic insights and itsanalytical application. Luminescence 28:821–826
25. Daneshfar A, Vafafard S (2009) Solubility of chloroquine diphosphate and 4,7-dichloroquinoline in water, ethanol, tetrahydrofuran, acetonitrile and acetone from (298.2 to 333.2) K. J Chem Eng Data 54:2170–2173
26. Renapurkar D (2011) Efficiency in chloroquine in management of chikungunya: a phase IV clinical trial. Intl J Pharma Bio Sci 2:407–412
27. Tariq M, Al-Badr A (1984) Chloroquine. In: Florey K (ed) Analytical profiles of drug substances. Academic, New York.pp, pp 95–125
28. Verbeeck RK, Junginger HE, Midha KK, Shah VP, Barends DM (2005) J Pharm Sci 94(7):1389–1394
29. Warwick C, Guerreiro A, Soares A (2013) Sensing and analysis of soluble phosphates in environmental samples: a review. Biosens Bioelectron 41:1–11
30. Idowu OR, Ajayi FO, Salako LA (1988) Specific spectrofluorimetric determination of chloroquine in blood plasma. Anal Chimca Acta 206:339–344
31. Liang Y, Song J, Yang X, Guo WA (2004) Flow-injection chemiluminescence determination of chloroquine using peroxynitrous acid as oxidant. Talanta 62:757–763
32. Niikura K, Metzger A, Anslyn E (1998) Chemosensor ensemble with selectivity for inositol-trisphosphate. J Am Chem Soc 120:8533–8534
33. Du J, Wang X, Jia M, Li T, Maoa J, Guo Z (2008) Recognition of phosphate anions in aqueous solution by a dinuclear zinc(II) complex of a cyclen-tethered terpyridine ligand. Inorg Chem Commun 11: 999–1002
34. Sun H, Scharff-Poulsen A, Gu H, Jakobsen I, Kossmann JM, Frommer WB, Almdal K (2008) Phosphate sensing by fluorescent reporter proteins embedded in polyacrylamide nanoparticles. ACS Nano 2(1):19–24
35. Wang F, Han M, Yi Mya K, Wang Y, Lai Y (2005) Aggregation-driven growth of size-tunable organic nanoparticles using electronically altered conjugated polymers. J Am Chem Soc 127: 10350–10355
36. Gore AH, Vatre SB, Anbhule PV, Han SH, Patil SR, Kolekar GB (2013) Direct detection of sulfide ions [S^{2-}] in aqueous mediabased onfluorescence quenching of functionalized CdSQDs at trace levels: analytical applications to environmental analysis. Analyst 138:1329–1333